Noninvasive Monitoring of Serial Changes in Pulmonary Vascular Resistance and Acute Vasodilator Testing Using Cardiac Magnetic Resonance

Ana García-Álvarez, Leticia Fernández-Friera, José Manuel García-Ruiz, Mario Nuño-Ayala, Daniel Pereda, Rodrigo Fernández-Jiménez, Gabriela Guzmán, Damián Sanchez-Quintana, Angel Alberich-Bayarri, David Pastor-Escuredo, David Sanz-Rosa, PHD, Jaime García-Prieto, Jesús G. Gonzalez-Mirelis, Gonzalo Pizarro Luis Jesús Jimenez-Borreguero, Valentín Fuster Javier Sanz Borja Ibáñez,

Objectives The study sought to evaluate the ability of cardiac magnetic resonance (CMR) to monitor acute and long-term changes in pulmonary vascular resistance (PVR) noninvasively.

Background PVR monitoring during the follow-up of patients with pulmonary hypertension (PH) and the response to vasodilator testing require invasive right heart catheterization.

Methods An experimental study in pigs was designed to evaluate the ability of CMR to monitor: 1) an acute increase in PVR generated by acute pulmonary embolization ($n = 10$); 2) serial changes in PVR in chronic PH ($n = 22$); and 3) changes in PVR during vasodilator testing in chronic PH ($n = 10$). CMR studies were performed with simultaneous hemodynamic assessment using a CMR-compatible Swan-Ganz catheter. Average flow velocity in the main pulmonary artery (PA) was quantified with phase contrast imaging. Pearson correlation and mixed model analysis were used to correlate changes in PVR with changes in CMR-quantified PA velocity. Additionally, PVR was estimated from CMR data (PA velocity and right ventricular ejection fraction) using a formula previously validated.

Results Changes in PA velocity strongly and inversely correlated with acute increases in PVR induced by pulmonary embolization ($r = -0.92$), serial PVR fluctuations in chronic PH ($r = -0.89$), and acute reductions during vasodilator testing ($r = -0.89$, $p \leq 0.01$ for all). CMR-estimated PVR showed adequate agreement with invasive PVR (mean bias −1.1 Wood units,; 95% confidence interval: −5.9 to 3.7) and changes in both indices correlated strongly ($r = 0.86$, $p < 0.01$).

Conclusions CMR allows for noninvasive monitoring of acute and chronic changes in PVR in PH. This capability may be valuable in the evaluation and follow-up of patients with PH. (J Am Coll Cardiol 2013;62:1621–31) © 2013 by the American College of Cardiology Foundation

Abbreviations and Acronyms

CMR = cardiac magnetic resonance

PA = pulmonary artery

PCWP = pulmonary capillary wedge pressure

PH = pulmonary hypertension

PVR = pulmonary vascular resistance

RHC = right heart catheterization

RV = right ventricular

WU = Wood units

Pulmonary vascular resistance (PVR) has important implications for the management and prognosis in patients with pulmonary hypertension (PH) (1) and chronic heart failure (2). Moreover, mean pulmonary artery (PA) pressure, and/or PVR response during acute vasodilator testing correlates with prognosis (3–5) and helps guiding physicians with the selection of appropriate therapy (1,6,7).

Currently, both acute vasodilator testing and PVR monitoring require invasive right heart catheterization (RHC). An accurate noninvasive alternative would be helpful to eliminate the discomfort, radiation exposure, and small but real risk of morbidity and mortality associated with RHC (8). Doppler echocardiography has become routine in the follow-up of patients with PH due to its ability to estimate systolic PA pressure, but has limited accuracy (9) and applicability (i.e., poor acoustic window or absence of tricuspid regurgitation) and it is not widely accepted for PVR estimation (10). Cardiac magnetic resonance (CMR) has been proposed as an alternative in assessing pulmonary hemodynamics noninvasively (11–15). It has been previously demonstrated that average PA flow velocity correlates strongly with PVR, and that CMR allows for noninvasive estimation of PVR values (16). However, whether CMR can accurately monitor serial changes in PVR is unknown. Therefore, our aim was to determine the ability of CMR to track acute and chronic fluctuations in PVR from serial changes in average PA velocity and CMR-estimated PVR.

Methods

Study design and experimental models. Experimental procedures were performed in castrated male Large-White pigs. The study was approved by the Institutional Animal Research Committee and carried out in compliance with the Guide for the Care and Use of Laboratory Animals. Before any procedure, anesthesia was induced by intramuscular injection of ketamine (20 mg/kg), xylazine (2 mg/kg), and midazolam (0.5 mg/kg), with buprenorphine (0.3 mg/kg) for analgesia, and the animals were intubated. All CMR and hemodynamic measures were obtained during spontaneous ventilation, anesthesia maintained with intravenous midazolam (0.2 mg/kg/h), and continuous electrocardiographic and oxymetric monitoring.

The ability of CMR to detect changes in PVR was evaluated under 3 different conditions:

1. Acute PH (n = 10), generated inside the magnet by pulmonary embolization with polydextrane-microspheres with a diameter of 300 μm (Sephadex G50, Pharmacia Biotech GmbH, Freiburg, Germany) (17) through the femoral vein. Each animal received a different dose from a suspension with 2.5 mg of microspheres per milliliter of saline (between 100 and 400 mg, median of 200 mg) in order to achieve a wide range of acute PH severity. CMR imaging with simultaneous hemodynamic monitoring was performed immediately pre- and post-embolization.
2. Chronic PH (n = 22), using 2 different models.

   Pre-capillary PH (n = 9) was generated with repeated microsphere embolization in a variant of a model previously described (18), using similar methodology as employed in the acute model but during mechanical ventilation. The first pulmonary embolization was performed in 3-month-old pigs (weight ≈40 kg) and repeated weekly until chronic stable PH was generated (mean PA pressure ≥25 mm Hg at rest). A median of 4 embolizations (range 3 to 6) with a median dose of microspheres of 500 mg was required to induce sustained PH.

   Post-capillary PH (n = 13) was generated by surgical nonrestrictive banding of the main pulmonary vein (venous confluent arising from the junction of both inferior pulmonary veins) through a small thoracotomy in 4-week-old piglets (weight ≈10 kg), a variant of a model previously described (19). This venous confluent drains both inferior pulmonary lobes, which account for ≈80% of total lung mass (Figs. 1A and 1B). Restriction of flow and secondary PH arise progressively as the animal grows. Animals were maintained with inhaled sevofluorane (1.5% to 2.0%) during the procedure under mechanical ventilation. The external jugular vein and internal carotid artery were dissected and cannulated for continuous recording of systemic and PA pressures. There was no perioperative mortality but 2 animals died suddenly during the follow-up period (2 and 3 months after the operation).CMR studies with simultaneous hemodynamic monitoring were performed at baseline, once chronic PH was generated, and every 4 weeks thereafter for 2 and 4 months, in the pre- and post-capillary models, respectively.
3. Acute vasodilator testing (n = 10 animals with chronic PH; 5 with pre- and 5 with post-capillary PH) was performed inside the magnet by increasing the inhaled oxygen concentration to 100% with all other conditions in steady state. CMR imaging with simultaneous hemodynamic monitoring was performed immediately before and 5 min after oxygen administration.

Invasive hemodynamic assessment. Hemodynamic measurements, obtained using a Swan-Ganz catheter via femoral or internal jugular vein, included mean PA pressure, pulmonary capillary wedge pressure (PCWP) at end-expiration, and cardiac output assessed by thermodilution. PVR was calculated as the difference between mean PA pressure and the estimated left atrial pressure divided by the cardiac output in Wood units

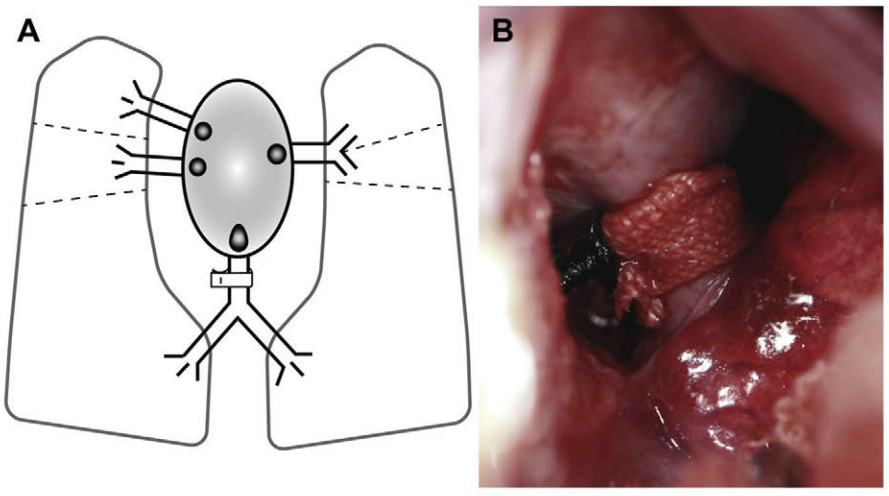

Figure 1 **Selective Nonrestrictive Banding of the Venous Confluent Draining Both Inferior Pulmonary Lobes**

(A) Diagram shows the anatomy of the pulmonary venous circulation and its drainage pattern into the left atrium in pigs. The inferior venous confluent has been encircled. **(B)** Surgical photograph showing the banding of the venous confluent at the exact resting diameter.

(WU). In animals with pre-capillary PH, PCWP was used as an estimate of left atrial pressure (mean difference between PCWP and left ventricular end-diastolic pressure of 0.8 mm Hg in a pilot study, N = 12), whereas in animals with post-capillary PH, left ventricular end-diastolic pressure quantified with a pigtail catheter was used, due to the variation of PCWP measurements amongst pulmonary lobes. Cardiac output and PVR were also indexed by body surface area estimated by the Brody's formula (20). Immediately after RHC, the Swan-Ganz catheter was replaced for a CMR-compatible version (Edwards, Irvine, California) and the animal was transferred to the CMR suite, adjacent to the catheterization laboratory.

CMR studies. CMR ACQUISITION. All CMR studies were performed with a 3.0-T magnet (Achieva-Tx, Philips Medical Systems, Best, the Netherlands), equipped with a 32-channel cardiac phased-array surface coil and retrospective electrocardiographic gating. Images were obtained with simultaneous monitoring of PA and systemic pressures using a CMR-compatible monitor (Invivo, Orlando, Florida). Steady-state free precession cine sequences were acquired in 10 to 15 contiguous short axis slices covering both ventricles from base to apex, and reconstructed into 25 cardiac phases each for the evaluation of ventricular volumes and function. Two-dimensional flow imaging (phase-contrast) was performed perpendicular to the main PA with a velocity-encoded gradient echo sequence using the minimum upper velocity limit without signal aliasing. For this purpose, 2 double-oblique orthogonal views oriented along the main axis of the PA trunk were acquired with a standard steady-state free precession cine sequence and used as the reference to prescribe a plane perpendicular to the main PA for the acquisition of phase-contrast images (Fig. 2). Similarly, 2D flow imaging in a cross-sectional view of the ascending aorta was obtained to determine left cardiac output. The following imaging parameters were applied for 2D flow imaging: repetition time/echo time 5.4/3.4 ms; number of averages 2; slice thickness 8 mm; voxel size 2.5 × 2.5 mm; reconstructed heart phases 40. In chronic PH animals, 2D flow imaging was performed at each visit. The agreement between cardiac output obtained by aortic 2D flow imaging and thermodilution was excellent (0.1 ± 0.4 l/min; $R = 0.92$, $p < 0.01$). Thus, in the acute models, where thermodilution could not be performed inside the magnet, cardiac output as assessed by phase-contrast of the aorta was used to compute PVR immediately before and after the intervention. In animals with chronic PH, 3D flow imaging on the main PA was additionally acquired.

CMR ANALYSIS. Short-axis steady-state cine and 2D phase-contrast acquisitions were analyzed using specialized software (Extended MR Workspace, Philips Medical Systems). Observers were blinded to the study arm and hemodynamic measurements. On cine images, biventricular endocardial contours were manually traced in end-diastole and end-systole and Simpson's method was used to calculate volumes and ejection fraction. Right ventricular (RV) trabeculations were included within the blood pool. Similarly, the inner contours of the main PA and aorta cross sections were outlined in each cardiac phase to quantify the average velocity during the complete cardiac cycle, minimum and maximum areas, and cardiac output. No phase-offset correction was performed, as the bias was negligible (data not shown). In a pilot study, we confirmed that the presence of the Swan-Ganz catheter inside the PA did not cause significant error in the estimation of average PA flow velocity (intraclass correlation coefficient of 0.95 and mean bias of 0.2 cm/s). PA elasticity was calculated as: (maximal area − minimal area)/minimal area × 100.

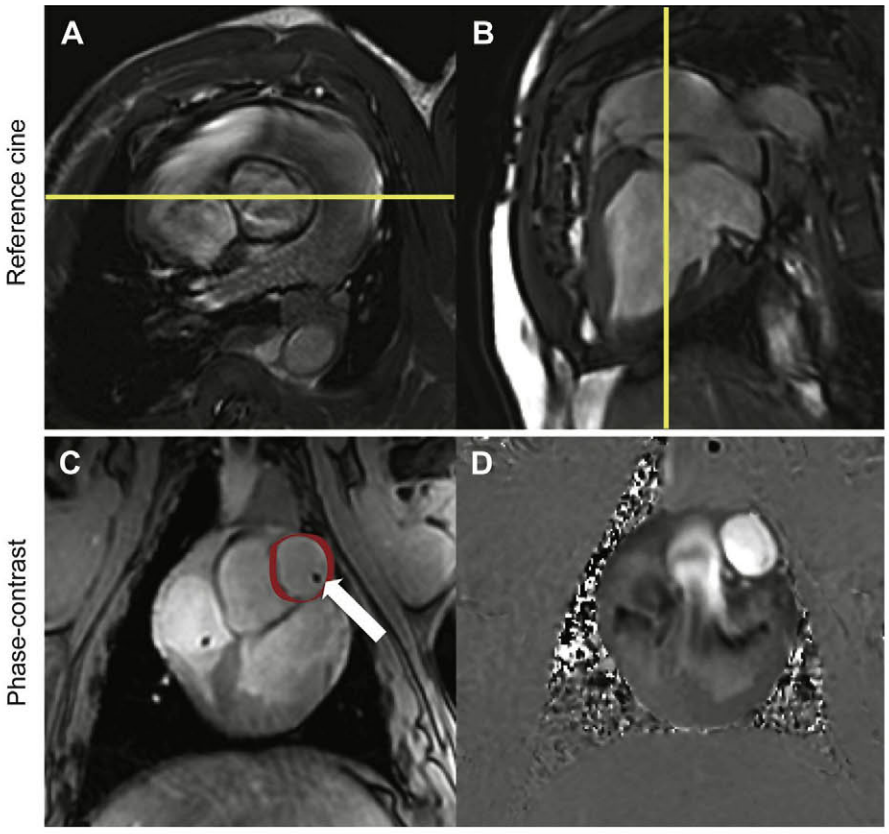

Figure 2 **Phase Contrast Imaging of the Main PA**

(A, B) Double-oblique orthogonal views oriented along the main axis **(yellow line)** of the pulmonary arterial (PA) trunk acquired with a steady-state free precession cine sequence. **(C, D)** Phase-contrast imaging on the main PA (**[C]** anatomic view, **[D]** flow-encoded view). **White arrow in C** represents Swan-Ganz catheter inside the pulmonary artery encircled in **red**.

CMR-estimated PVR was calculated using the formula previously validated (16) as: PVR (WU) = 19.38 − [4.62 × ln PA velocity (cm/s)] − [0.08 × RV ejection fraction (%)]. 3D-phase-contrast acquisitions were analyzed using GTFlow package (Gyrotools Inc., Zurich, Switzerland). PA was segmented semiautomatically using morphological operators and blood flow pathlines were generated for the qualitative assessment of flow patterns and detection of vortices (21).

Histopathology. At the completion of the study, animals with chronic PH were euthanized with a lethal injection of pentobarbital sodium and the heart, PA, and lung parenchyma were excised. Macroscopic high-resolution photographs were taken using a digital camera. Standard hematoxylin and eosin staining, and picrosirius red and Masson's trichrome staining were performed to evaluate microscopic changes and the presence of collagen in order to demonstrate typical lesions in the chronic PH models. A stereomicroscope Nikon SMZ 1500 (Nikon Instruments Inc., Melville, New York) was used.

Statistical analysis. Continuous variables are expressed as median (interquartile range or range). For the evaluation of serial changes in PVR (second condition), average PA velocity was natural logarithm-transformed because its association with PVR in chronic PH is curvilinear, as previously described (16). Correlation between acute changes in PA velocity and PVR induced by pulmonary embolization or vasodilator testing was assessed using Pearson correlation. Mixed model analysis with correction for repeated measurements was used to correlate changes in PVR and changes in PA velocity in chronic PH, and to develop an equation to predict the change in PVR per percent change in PA velocity. Changes in PVR and PA velocity in chronic PH were calculated as the difference between measurements in 2 consecutive follow-up visits. Changes in PA velocity and PVR were further dichotomized to assess sensitivity, specificity, and positive and negative predictive values of a reduction of PA velocity to detect an increase in PVR. Analyses were performed using STATA version 12 (StataCorp LP, College Station, Texas) and SPSS version 20 (IBM Corp., Armonk, New York).

Results

Ability of CMR to track changes in PVR. ACUTE PH. Acute pulmonary embolization caused an increase in PVR (median

Table 1 Changes in Hemodynamic and Phase Contrast Parameters During Acute Embolization

	Baseline	Post-Embolization	Change	p Value
Heart rate, beats/min	76.0 (14.0)	80.5 (24.0)	2.0 (−14 to 27)	0.39
Oxygen saturation, %	97.5 (5.0)	94.5 (16.0)	−3.5 (−24 to 6)	0.12
Mean BP, mm Hg	92.0 (26.0)	85.5 (33.25)	−6.5 (−43 to 7)	0.07
Mean PA pressure, mm Hg	18.0 (10.0)	37.5 (12.0)	17.5 (5.0 to 32.0)	<0.01
Cardiac output, l/min	3.7 (1.7)	2.7 (1.3)	−0.7 (−2.7 to 0.5)	0.02
PCWP, mm Hg	11.5 (3.0)	11.5 (4.3)	0 (−1 to −1)	1.00
PVR, Wood units	1.8 (2.2)	10.0 (4.9)	6.8 (1.4 to 11.7)	<0.01
PA flow velocity, cm/s	13.5 (6.5)	8.5 (3.9)	4.9 (0.1 to 11.0)	<0.01
PA minimal area, cm^2	3.6 (1.3)	5.6 (2.8)	1.6 (0.2 to 3.8)	<0.01
PA elasticity, %	28.6 (24.5)	15.1 (11.4)	−9.6 (−38 to 7)	0.04

Values at baseline and post-embolization are median (interquartile range) and change is expressed as median (minimum to maximum).
BP = blood pressure; IQR = interquartile range; PA = pulmonary artery; PCWP = pulmonary capillary wedge pressure; PVR = pulmonary vascular resistance.

6.8 WU; range 1.4 to 11.7 WU) and mean PA pressure (median 17.5 mm Hg; range 5 to 32 mm Hg) with a reduction in cardiac output (median 0.7 l/min; range 0 to 2.7 l/min). These hemodynamic changes were accompanied by a significant decrease in PA velocity, an increase in PA area, and a reduction in PA elasticity (Table 1).

The magnitude of the fall in PA velocity strongly correlated with the increment in PVR ($r = -0.92$, $p < 0.001$) (Fig. 3A). The change in PVR moderately correlated with the change in PA elasticity ($r = -0.63$, $p = 0.05$) and did not correlate with the change in PA area ($r = 0.30$, $p = 0.39$).

CHRONIC PH. Baseline and follow-up characteristics of the chronic PH animals are shown in Tables 2 and 3.

An increase in cardiac output along the follow-up related with animal growth was observed in both models. Changes in PVR between follow-up visits were greater in the post-capillary model compared to the pre-capillary model (median 0.5 WU [range −5.4 to 19.0 WU] vs. median 0.1 WU [range −2.5 to 2.6 WU], respectively; $p = 0.08$).

Serial changes in between-visits PA velocity by CMR strongly correlated with changes in PVR ($r = -0.89$, $p < 0.01$) (Fig. 3B). According to the equation obtained: change in PVR (WU) = −0.2 − 11.2 × change in ln[PA velocity (cm/s)], it can be estimated that average PVR increased approximately 1 WU for each 10% decrease in PA velocity. Subgroup analysis showed better correlation in the post-capillary than the pre-capillary model ($r = -0.92$, $p < 0.01$ vs. $r = -0.76$, $p < 0.01$; p value for the interaction <0.01). Figure 4 shows some examples of the evolution of PVR and PA velocity during follow-up. Sensitivity, specificity, positive predictive value, and negative predictive values for a reduction in PA velocity to detect an increase in PVR were 86%, 70%, 79%, and 79%, respectively. Serial changes in between-visits PVR moderately correlated with changes in PA area ($r = 0.61$, $p < 0.01$) and changes in PA elasticity ($r = -0.50$, $p < 0.01$). Serial changes in between-visits PA velocity by CMR also correlated well with changes in indexed PVR ($r = -0.82$, $p < 0.01$). Animal weight and heart rate did not behave as confounders on the association between changes in PA velocity and PVR.

The concordance between absolute values of invasive PVR and CMR-estimated PVR during follow-up using the previously published formula (that includes average PA

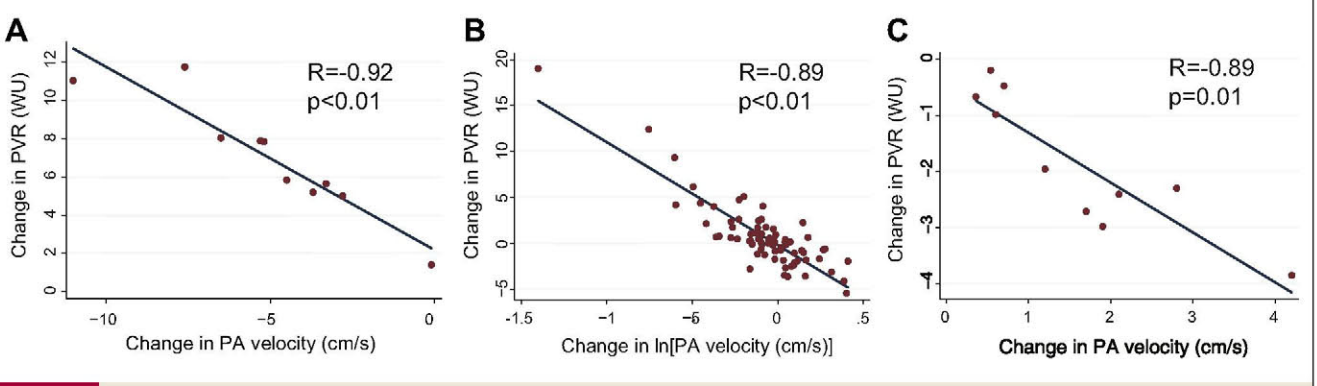

Figure 3 Correlation Between Changes in PVR and Changes in Average PA Velocity in the 3 Different Conditions

(A) Acute pulmonary embolization, **(B)** chronic pulmonary hypertension, **(C)** acute vasodilator testing. PA = pulmonary artery; PVR = pulmonary vascular resistance; WU = Wood units.

Table 2 Baseline and Follow-Up Characteristics of Chronic Pre-Capillary PH Group

		Chronic PH		
	Baseline	At Generation	After 1 Month	After 2 Months
Weight, kg	40.0 (15.0)	55.0 (16.0)	68.5 (4.0)	81.0 (4.0)
Body surface area, m^2	1.0 (0.23)	1.2 (0.2)	1.4 (0.1)	1.6 (0.05)
Heart rate, beats/min	75.0 (8.0)	75.0 (16.0)	70.0 (10.0)	74.0 (13.0)
Oxygen saturation, %	94.0 (6.0)	90.0 (2.0)	94.0 (3.0)	92.0 (3.0)
Mean BP, mm Hg	97.0 (9.0)	95.0 (16.0)	97.0 (9.0)	103 (9.0)
Mean PA pressure, mm Hg	21.0 (9.0)	28.0 (3.0)	27.0 (5.0)	27.0 (3.0)
Cardiac output, l/min	4.3 (1.0)	6.2 (1.1)	6.0 (1.6)	7.2 (1.4)
Cardiac index, l/min/m^2	4.1 (0.6)	4.6 (0.7)	4.3 (0.8)	4.6 (0.5)
PCWP, mm Hg	9.0 (1.0)	12.0 (5.0)	10.0 (4.0)	13.0 (8.0)
PVR, Wood units	2.3 (1.4)	2.7 (1.3)	2.7 (2.2)	2.2 (1.1)
PVR index, Wood units•m^2	2.9 (1.8)	3.1 (1.6)	3.4 (0.7)	3.2 (1.5)
Average PA velocity, cm/s	11.0 (2.8)	11.6 (2.5)	11.7 (3.2)	10.9 (1.8)
PA minimal area, cm^2	5.4 (2.1)	6.3 (0.7)	7.2 (1.0)	8.0 (1.4)
PA elasticity, %	32.3 (10.7)	36.9 (5.1)	37.7 (6.2)	30.0 (7.1)

Values are median (interquartile range).
PH = pulmonary hypertension; other abbreviations as in Table 1.

velocity and RV ejection fraction) (16) was adequate ($r = 0.83$, $p < 0.01$; mean bias of −1.1 WU and limits of agreement of −5.9 and 3.7 WU). Serial changes in CMR-estimated PVR and changes in invasive PVR showed a good concordance as well ($r = 0.86$, $p < 0.01$; mean bias of −0.14 WU and limits of agreement of −4.7 and 4.4 WU), although a trend to underestimate large PVR changes was observed (Fig. 5).

In addition to changes in quantitative parameters, the appearance of vortices in the flow of the main PA could be identified with 3D phase-contrast imaging in all animals with chronic PH (Fig. 6, Online Videos 1 and 2).

ACUTE VASODILATOR TESTING. Oxygen administration caused a reduction in PVR (median −2.1 WU, range −3.8 to 0.2 WU) and mean PA pressure (median −7.0 mm Hg, range −15 to 1 mm Hg), without significant changes in cardiac output (median 0.0 l/m, range −0.8 to 0.5 l/min). These hemodynamic changes were accompanied by a significant increase in PA velocity, an increase in PA elasticity, and a reduction in PA area (Table 4).

The change in PA velocity strongly correlated with the reduction in PVR ($r = -0.89$, $p = 0.01$) (Fig. 3C) and mean PA pressure ($r = -0.86$, $p = 0.02$). Baseline PA elasticity (before vasodilator testing) significantly correlated with the change in PVR ($r = 0.73$, $p = 0.04$) but the acute change in PVR did not correlate with the acute change in PA area or elasticity.

Histopathologic examination. Chronic PH generation was associated in both experimental models with typical changes of arterial intimal proliferation, hypertrophy of the media and perivascular fibrosis of vessels inside the lung, hypertrophy and increased collagen deposition in the media

Table 3 Baseline and Follow-Up Characteristics of Chronic Post-Capillary PH Group

	Baseline	1 Month	2 Months	3 Months	4 Months
Weight, kg	12.5 (2.0)	22.5 (3.0)	40.0 (10.5)	57.3 (11.0)	80.5 (5.5)
BSA, m^2	0.5 (0.05)	0.7 (0.06)	1.0 (0.2)	1.3 (0.1)	1.6 (0.1)
Heart rate, beats/min	120.0 (21.0)	98.0 (18.0)	74.0 (14.0)	68.0 (9.5)	62.0 (11.0)
Oxygen saturation, %	99.0 (1.0)	90.0 (11.0)	91.0 (6.0)	93.0 (4.0)	95.0 (3.0)
Mean BP, mm Hg	57.0 (8.0)	77.0 (15.0)	92.5 (17.5)	93.5 (12.5)	91.0 (7.0)
Mean PA pressure, mm Hg	19.0 (3.0)	30.0 (10.0)	36.0 (14.0)	34.5 (14.0)	35.0 (8.0)
Cardiac output, l/min	1.9 (0.6)	3.3 (0.8)	4.4 (1.4)	5.9 (1.0)	6.8 (2.7)
Cardiac index, l/min/m^2	3.6 (0.8)	4.8 (1.1)	4.3 (1.0)	4.3 (0.7)	4.3 (1.1)
LVEDP, mm Hg	14.0 (2.0)*	6.0 (3.0)	8.0 (2.0)	9.0 (3.5)	9.0 (4.0)
PVR, Wood units	2.5 (1.4)	6.7 (1.5)	7.1 (4.6)	4.0 (2.1)	3.7 (1.0)
PVR index, Wood units•m^2	1.0 (0.6)	4.2 (1.1)	6.4 (5.2)	5.8 (3.2)	6.2 (2.2)
Average PA velocity, cm/s	14.7 (1.9)	11.0 (3.0)	11.0 (2.9)	11.4 (1.8)	11.5 (2.9)
PA minimal area, cm^2	1.8 (0.3)	3.7 (1.2)	5.4 (2.1)	6.3 (1.9)	7.8 (1.3)
PA elasticity, %	42.9 (12.1)	21.2 (10.8)	32.5 (8.3)	35.2 (19.0)	31.6 (21.2)

Values are median (interquartile range). *Pulmonary wedge pressure at end-expiration was used instead of EDLVP at baseline.
BSA = body surface area; LVEDP = left ventricular end-diastolic pressure; other abbreviations as in Tables 1 and 2.

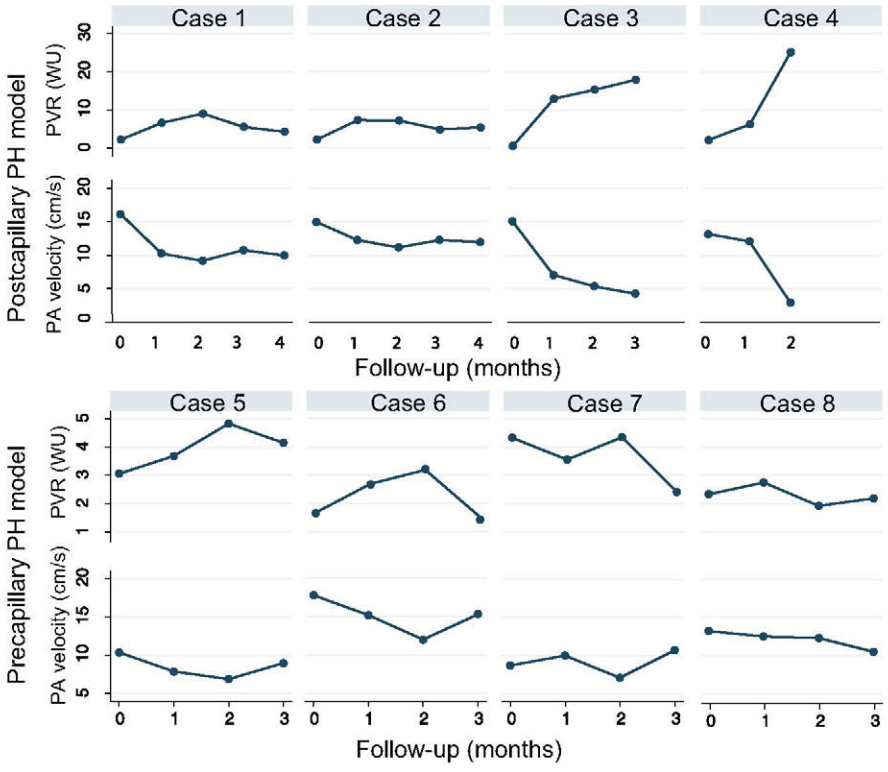

Figure 4 **Example of 8 Cases of Chronic PH**

Cases illustrating the concordance between the evolution of pulmonary vascular resistance and average pulmonary artery velocity during the follow-up. PH = pulmonary hypertension; other abbreviations as in Figure 3.

of the main PA, and RV dilatation, hypertrophy and myocardial fibrosis and disarray (Fig. 7).

Discussion

The main findings of this study are the following: 1) CMR allows noninvasive monitoring of serial changes in PVR in chronic PH; 2) semiquantitative monitoring can be performed by determining simple changes in average PA flow velocity; and 3) variations in average PA velocity additionally have the ability to track acute increases or decreases in PVR.

PVR monitoring by RHC is recommended in patients with chronic PH and those with heart failure awaiting heart transplantation (2). It has been recently reported that

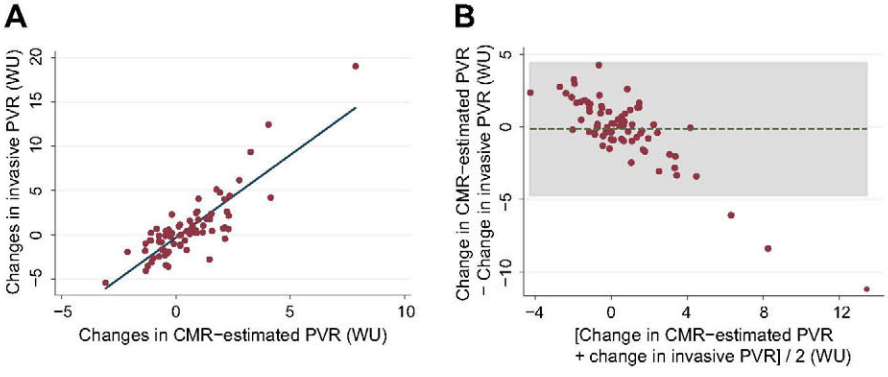

Figure 5 **Diagnostic Accuracy of the CMR Formula to Monitor Changes in PVR**

Correlation **(A)** and Bland-Altman plot **(B)** showing the association between changes in PVR as assessed by right heart catheterization (invasive PVR) and changes in PVR estimated based on cardiac magnetic resonance (CMR) data (CMR-quantified PVR). Abbreviations as in Figure 3.

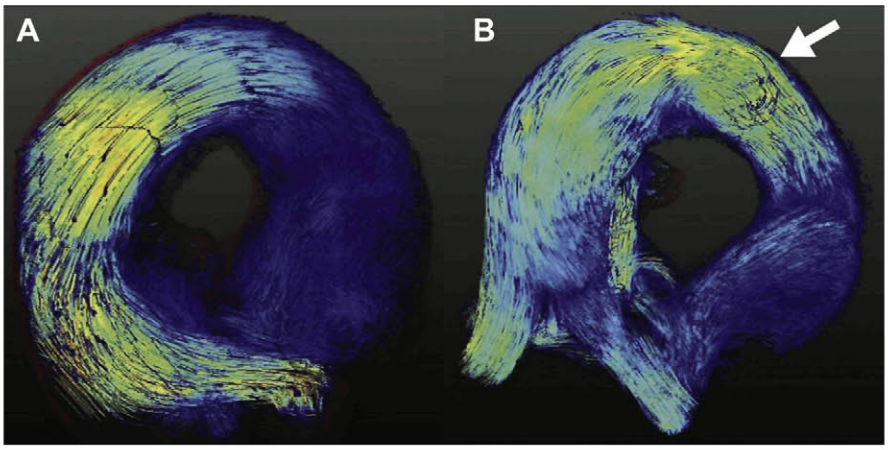

Figure 6 **Three-Dimensional Phase Contrast Imaging of the Main Pulmonary Artery**

(A) Control animal without pulmonary hypertension showing laminar flow. **(B)** Case of post-capillary pulmonary hypertension showing turbulent flow and formation of a flow vortex in the main pulmonary artery **(arrow)**. Please see Online Videos 1 and 2.

a method combining the average PA velocity and RV ejection fraction, both measured by CMR, allowed noninvasive estimation of PVR in patients with chronic PH at a single time point (16). In the present study we further evaluated whether this approach would be able to monitor serial changes in PVR, and therefore its potential for noninvasive follow-up, in experimental models of chronic PH. The 2 models employed led to the expected abnormalities not only in hemodynamics but also in cardiovascular adaptation to chronic pressure overload, as confirmed by the changes in the heart and pulmonary artery demonstrated in histopathological analyses (Fig. 7). Overall, PVR tended to increase initially and stabilize during follow-up. However, some subjects showed reduction of PVR between visits due to adaptation mechanisms, which allowed us to evaluate the accuracy of CMR to track changes in PVR on both directions. This mimics clinical PH, with between-visits PVR increase due to disease progression or reduction with treatment. We were able to replicate the accuracy of the previously reported CMR method (16) in this experimental setting again with narrower limits of agreement than those reported with echocardiography (10,22,23) and, most importantly, demonstrate its ability to track variations in PVR over time.

The combination of RV ejection fraction and average PA velocity enables absolute quantification of PVR; however, it also adds complexity and scanning time. Based on previous studies (15,16), we focused on changes in average PA velocity alone as an alternative method, as this was the parameter with the strongest correlations with PVR and the highest weight in the predictive model. In addition, PA velocity can be easily and rapidly quantified, and is more likely to reveal acute changes in hemodynamic conditions than parameters that reflect structural adaptation to chronic PH such as RV ejection fraction or PA dimensions. The presence of low PA velocities by CMR in patients with chronic PH has been long recognized (24,25). There are several mechanisms that may contribute to the tight relation between changes in PVR and changes in PA flow velocity. Increased PVR in chronic PH is associated with vasoconstriction and remodeling of distal vessels, so blood transit

Table 4 **Changes in Hemodynamic and Phase Contrast Parameters During Vasodilator Testing**

	Baseline	Post-Vasodilator Test	Change	p Value
Heart rate, beats/min	73.5 (21.0)	74.5 (23.0)	−6.0 (−14.0 to 12.0)	0.15
Oxygen saturation, %	89.0 (5.0)	98 (2.0)	10.0 (6.0 to 18.0)	<0.01
Mean BP, mm Hg	85.5 (34.0)	95.0 (49.7)	0.5 (−9 to 22)	0.61
Mean PA pressure, mm Hg	36.5 (14.0)	27.5 (19.0)	−7.0 (−15.0 to −1.0)	<0.01
Cardiac output, l/min	4.7 (2.1)	4.5 (2.5)	0.0 (−0.8 to 0.5)	0.88
PCWP, mm Hg	9.0 (5.0)	8.2 (5.0)	−0.2 (−1 to 0)	1.00
PVR, Wood units	4.9 (2.8)	3.4 (4.1)	−2.1 (−3.8 to −0.2)	<0.01
PA flow velocity, cm/s	9.8 (2.4)	11.9 (3.1)	1.5 (0.4 to 4.2)	<0.01
PA minimal area, cm^2	5.8 (3.9)	4.3 (3.7)	−1.2 (−1.8 to −0.6)	0.01
PA elasticity, %	28.2 (14.0)	34.2 (24.8)	9.7 (−32 to 5)	0.04

Values at baseline and post-vasodilator test are median (interquartile range) and change is expressed as median (minimum to maximum).
Abbreviations as in Table 1.

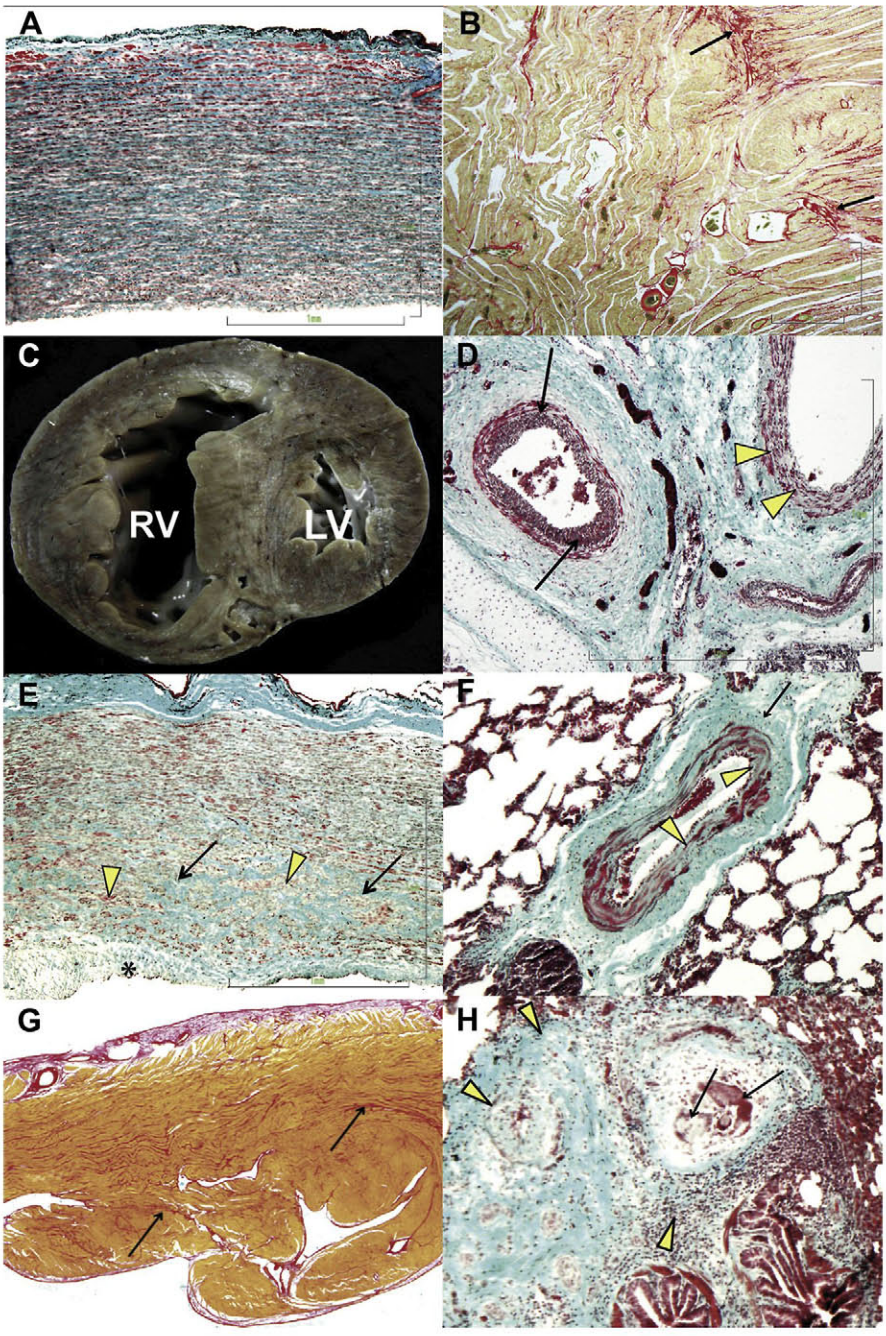

Figure 7 **Example of Pathology Changes in a Case of Post-Capillary PH and in a Case of Pre-Capillary PH**

(A) Masson's trichrome staining showing increased collagen fibers in the tunica media of the main pulmonary artery (PA). **(B)** Picrosirius red staining of the right ventricular (RV) free wall showing myocardial disarray and fibrosis **(arrows)**. **(C)** Cross section of the heart showing marked RV hypertrophy and dilatation. **(D)** Masson's trichrome staining showing arterial intimal proliferation **(arrows)** and hypertrophy of the media **(arrowheads)** in the middle pulmonary lobe. **(E)** Masson's trichrome staining showing increased collagen fibers in the media of the main PA **(arrow)**, disarray of smooth muscle cells **(arrowheads)**, and intimal fibrosis **(asterisk)**. **(F)** Masson's trichrome staining showing arterial medial hypertrophy and crescent-like fibrous intimal cushion **(arrowheads)** that causes luminal narrowing and adventitial thickening **(arrows)**. **(G)** Picrosirius red staining of the RV free wall showing myocardial fibrosis **(arrows)**. **(H)** Masson's trichrome staining showing adventitial thickening and vasculitis with transmural infiltration of lymphocytes **(arrowheads)**. Obliteration, fibrosis, and recanalization of a thrombosed pulmonary artery **(arrows)**. LV = left ventricle; PH = pulmonary hypertension.

through the pulmonary tree is hampered. Increased PVR subsequently causes PA dilatation and associated changes of flow pattern characterized by the presence of systolic retrograde flow (24) and the formation of flow vortices (21) (as shown in Fig. 6, Online Videos 1 and 2). Finally, as PH progresses, the RV fails and cardiac output tends to decrease.

The combination of all these mechanisms causes, for any given flow and PA pressure, a reduction in average velocity. In contrast with other techniques such as Doppler echocardiography or catheter-tip velocity transducer, CMR allows for average flow velocity from the complete PA cross-sectional area through the entire cardiac cycle avoiding the wrong assumption of a uniform PA flow profile.

For the objective of monitoring changes in PVR during follow-up, PA velocity alone performed as well as the more complex method and is significantly simpler. As additional advantages, 2D flow imaging is easily acquired during free breathing, does not require contrast agent administration, and is easily processed with high intraobserver and interobserver reproducibility (16). Correlations with PVR variations were stronger in the post-capillary compared to the pre-capillary model, probably because the range of PVR changes was wider. In a prior small study of chronic PH patients with serial RHC and CMR performed at 2 different time points, it was observed that changes in PA velocities or dimensions differed between patients who experienced hemodynamic improvement during follow-up (26). Our present study with simultaneous hemodynamic assessment strengthens this observation without the limitations of performing tests on different days with potential significant variations in PVR. Based on our results, we believe that in the presence of clinical stability and RV function stability (as can be accurately assessed by CMR), an increase or maintenance of average PA velocity could serve to delay or space RHC studies. Further studies will help to elucidate the precise role that CMR may play to monitor patients with chronic PH.

A previous study (27) showed that PA distensibility, as assessed by CMR, was significantly higher in patients with a positive response in vasodilator testing performed within 48 h. To our knowledge, ours is the first study of simultaneous CMR imaging and hemodynamic invasive assessment during acute vasodilator testing. Beyond the ability to detect serial PVR changes in chronic PH, we confirmed the hypothesized dynamic response of PA velocity to hemodynamic conditions and demonstrated strong correlations between acute fluctuations in average PA velocity and PVR. Consequently, another interesting and potential application of noninvasive PVR monitoring with CMR could be the evaluation of pulmonary vascular reactivity. Our results suggest that vasodilator testing could be incorporated into the comprehensive CMR study of chronic PH patients. Several medications might be used as vasodilators. We decided to use high oxygen dose due to its availability, easy administration, safety, and demonstrated effect in experimental PH models (18). Moreover, oxygen has been traditionally used for vasodilator testing in pediatric patients (28), a population especially attractive to conduct noninvasive evaluation avoiding radiation and instrumentation.

Study limitations. Some limitations of this investigation should be acknowledged. CMR-compatible Swan-Ganz catheters do not have thermistor, so the value of cardiac output used for the calculation of PVR during CMR in the acute models was not derived from thermodilution (the gold standard) but from phase-contrast imaging. However, phase-contrast is well validated and we could demonstrate an excellent correlation between both techniques when thermodilution was performed immediately before imaging and all conditions were steady state. We applied the temporal resolution typically used in clinical evaluations as a compromise between quality and acquisition time. The pre-capillary PH model generated by repeated pulmonary embolizations created only mild PH as compared with the post-capillary model. Although it was helpful to evaluate the behavior of serial cardiac MR imaging with mild changes or stability of PVR and to test the CMR method in 2 different models of chronic PH, it has to be recognized that PH severity was low in the pre-capillary model. Related with this issue, the range of PVR changes along the follow-up was narrower, which may explain the lower correlation between changes in PVR and PA velocity, as compared with the post-capillary model. Further studies are needed to evaluate the utility of noninvasive CMR monitoring in patients with severe pre-capillary PH and to confirm the correlation between acute change in average PA velocity and acute reduction in PVR using other vasodilators such as nitric oxide or epoprostenol.

Conclusions

CMR allows noninvasive monitoring of serial changes of PVR in chronic PH and the acute response of PVR during vasodilator testing. This may be of great value in the evaluation and follow-up of patients with chronic PH.

Acknowledgments

Gonzalo J. Lopez and Angel Macias were capital for the high-quality CMR examinations. Tamara Córdoba, Eugenio Fernández, and the rest of the people working in the animal facilities and CNIC's farm were outstanding in animal care and unconditional support. Antonio de Molina helped with histological analyses in our pilot studies. The authors thank Iñigo Sanz for his outstanding surgical pictures, and María J. Ledesma-Carbayo for her dedication and expertise in the analysis of 3D flow imaging.

Reprint requests and correspondence: Dr. Borja Ibáñez, Imaging in Experimental Cardiology Laboratory (IExC Lab), Epidemiology, Atherothrombosis and Imaging Department, Centro Nacional de Investigaciones Cardiovasculares Carlos III (CNIC), Melchor Fernández Almagro 3, 28029 Madrid, Spain. E-mail: bibanez@cnic.es.

REFERENCES

1. McLaughlin VV, Archer SL, Badesch DB, et al. ACCF/AHA 2009 expert consensus document on pulmonary hypertension a report of the American College of Cardiology Foundation Task Force on Expert Consensus Documents and the American Heart Association developed in collaboration with the American College of Chest Physicians;

American Thoracic Society, Inc.; and the Pulmonary Hypertension Association. J Am Coll Cardiol 2009;53:1573–619.
2. Mehra MR, Kobashigawa J, Starling R, et al. Listing criteria for heart transplantation: International Society for Heart and Lung Transplantation guidelines for the care of cardiac transplant candidates—2006. J Heart Lung Transplant 2006;25:1024–42.
3. Costard-Jackle A, Fowler MB. Influence of preoperative pulmonary artery pressure on mortality after heart transplantation: testing of potential reversibility of pulmonary hypertension with nitroprusside is useful in defining a high risk group. J Am Coll Cardiol 1992;19:48–54.
4. Raffy O, Azarian R, Brenot F, et al. Clinical significance of the pulmonary vasodilator response during short-term infusion of prostacyclin in primary pulmonary hypertension. Circulation 1996;93:484–8.
5. Sitbon O, Humbert M, Jais X, et al. Long-term response to calcium channel blockers in idiopathic pulmonary arterial hypertension. Circulation 2005;111:3105–11.
6. Beyersdorf F, Schlensak C, Berchtold-Herz M, Trummer G. Regression of "fixed" pulmonary vascular resistance in heart transplant candidates after unloading with ventricular assist devices. J Thorac Cardiovasc Surg 2010;140:747–9.
7. McMurray JJ, Adamopoulos S, Anker SD, et al. ESC Guidelines for the diagnosis and treatment of acute and chronic heart failure 2012: the Task Force for the Diagnosis and Treatment of Acute and Chronic Heart Failure 2012 of the European Society of Cardiology. Developed in collaboration with the Heart Failure Association (HFA) of the ESC. Eur Heart J 2012;33:1787–847.
8. Hoeper MM, Lee SH, Voswinckel R, et al. Complications of right heart catheterization procedures in patients with pulmonary hypertension in experienced centers. J Am Coll Cardiol 2006;48:2546–52.
9. Fisher MR, Forfia PR, Chamera E, et al. Accuracy of Doppler echocardiography in the hemodynamic assessment of pulmonary hypertension. Am J Respir Crit Care Med 2009;179:615–21.
10. Rajagopalan N, Simon MA, Suffoletto MS, et al. Noninvasive estimation of pulmonary vascular resistance in pulmonary hypertension. Echocardiography 2009;26:489–94.
11. Bell A, Beerbaum P, Greil G, et al. Noninvasive assessment of pulmonary artery flow and resistance by cardiac magnetic resonance in congenital heart diseases with unrestricted left-to-right shunt. J Am Coll Cardiol Img 2009;2:1285–91.
12. Laffon E, Vallet C, Bernard V, et al. A computed method for noninvasive MRI assessment of pulmonary arterial hypertension. J Appl Physiol 2004;96:463–8.
13. Mousseaux E, Tasu JP, Jolivet O, Simonneau G, Bittoun J, Gaux JC. Pulmonary arterial resistance: noninvasive measurement with indexes of pulmonary flow estimated at velocity-encoded MR imaging—preliminary experience. Radiology 1999;212:896–902.
14. Nogami M, Ohno Y, Koyama H, et al. Utility of phase contrast MR imaging for assessment of pulmonary flow and pressure estimation in patients with pulmonary hypertension: comparison with right heart catheterization and echocardiography. J Magn Reson Imaging 2009;30:973–80.
15. Sanz J, Kuschnir P, Rius T, et al. Pulmonary arterial hypertension: noninvasive detection with phase-contrast MR imaging. Radiology 2007;243:70–9.
16. Garcia-Alvarez A, Fernandez-Friera L, Mirelis JG, et al. Non-invasive estimation of pulmonary vascular resistance with cardiac magnetic resonance. Eur Heart J 2011;32:2438–45.
17. Bottiger BW, Motsch J, Dorsam J, et al. Inhaled nitric oxide selectively decreases pulmonary artery pressure and pulmonary vascular resistance following acute massive pulmonary microembolism in piglets. Chest 1996;110:1041–7.
18. Weimann J, Zink W, Gebhard MM, Gries A, Martin E, Motsch J. Effects of oxygen and nitric oxide inhalation in a porcine model of recurrent microembolism. Acta Anaesthesiol Scand 2000;44:1109–15.
19. LaBourene JI, Coles JG, Johnson DJ, Mehra A, Keeley FW, Rabinovitch M. Alterations in elastin and collagen related to the mechanism of progressive pulmonary venous obstruction in a piglet model. A hemodynamic, ultrastructural, and biochemical study. Circ Res 1990;66:438–56.
20. Brody S. A comparison of growth curves of man and other animals. Science 1928;67:43–6.
21. Reiter G, Reiter U, Kovacs G, et al. Magnetic resonance-derived 3-dimensional blood flow patterns in the main pulmonary artery as a marker of pulmonary hypertension and a measure of elevated mean pulmonary arterial pressure. Circ Cardiovasc Imaging 2008;1:23–30.
22. Haddad F, Zamanian R, Beraud AS, et al. A novel non-invasive method of estimating pulmonary vascular resistance in patients with pulmonary arterial hypertension. J Am Soc Echocardiogr 2009;22:523–9.
23. Scapellato F, Temporelli PL, Eleuteri E, Corra U, Imparato A, Giannuzzi P. Accurate noninvasive estimation of pulmonary vascular resistance by Doppler echocardiography in patients with chronic failure heart failure. J Am Coll Cardiol 2001;37:1813–9.
24. Bogren HG, Klipstein RH, Mohiaddin RH, et al. Pulmonary artery distensibility and blood flow patterns: a magnetic resonance study of normal subjects and of patients with pulmonary arterial hypertension. Am Heart J 1989;118:990–9.
25. Kondo C, Caputo GR, Masui T, et al. Pulmonary hypertension: pulmonary flow quantification and flow profile analysis with velocity-encoded cine MR imaging. Radiology 1992;183:751–8.
26. Dellegrottaglie S, Perrone-Filardi P, Garcia-Alvarez A, et al. Serial phase-contrast MRI for prediction of pulmonary hemodynamic changes in patients with pulmonary arterial hypertension. Int J Cardiol 2012;157:140–2.
27. Jardim C, Rochitte CE, Humbert M, et al. Pulmonary artery distensibility in pulmonary arterial hypertension: an MRI pilot study. Eur Respir J 2007;29:476–81.
28. Marshall HW, Swan HJ, Burchell HB, Wood EH. Effect of breathing oxygen on pulmonary artery pressure and pulmonary vascular resistance in patients with ventricular septal defect. Circulation 1961;23:241–52.

Key Words: magnetic resonance ■ monitoring ■ pulmonary hypertension ■ pulmonary vascular resistance ■ vasodilator testing.